Article

Correlating Cutting Performance and Surface Roughness under Different Bias Using TiAlTaN Coated Milling Tools

Gustavo F. Pinto [1,2,*], David Almeida [1], Francisco J. G. Silva [1,2], Eduardo Silva [4],
Ricardo Alexandre [5], Filipe Fernandes [1,3] and Andresa Baptista [1,2]

[1] CIDEM, ISEP, Polytechnic of Porto, Rua Dr. António Bernardino de Almeida, 4249-015 Porto, Portugal
[2] LAETA-INEGI, Associate Laboratory for Energy, Transports and Aerospace, Rua Dr. Roberto Frias 400,
    4200-465 Porto, Portugal
[3] Department of Mechanical Engineering, ARISE, CEMMPRE, University of Coimbra, Rua Luís Reis Santos,
    3030-788 Coimbra, Portugal
[4] Durit Coatings, S.A., Pq. Industrial de Taveiro, 3045-504 Taveiro, Portugal
[5] Inovatools Portugal Unip. Lda, R. da Indústria Metalúrgica 593, 2430-528 Marinha Grande, Portugal
* Correspondence: gflp@isep.ipp.pt; Tel.: +351-22-83-40-500

Abstract: Driven by the industry's ongoing pursuit of continuous improvement in machining processes, the need to meet environmental targets, and the limited number of scientific studies addressing coatings doped with Tantalum (Ta), were the main motivations to undertake this investigation. This study investigates the impact of coating cutting tools with a TiAlTaN film deposited at two different bias voltages, −90 V and −135 V, and its relationship with cutting forces, surface roughness, and overall performance when machining AISI P20 steel. The choice of AISI P20 steel was deliberate, considering its widespread use in the mould manufacturing industry and the machining challenges posed by its mechanical properties. Throughout the study, during the machining process, the cutting forces in the three axes were measured, as well as the surface roughness of the AISI P20 steel after machining. A correlation was made between the cutting forces obtained and the roughness of the machined surface, considering the coated tools using bias of −90 V and −135 V. The results show that increasing bias level during the coating deposition has a positive effect on the tool machining performance. Also, there was a correlation between the cutting forces during the machining process and the surface roughness of the machined AISI P20 steel. The coated tool with −135 V bias induced lower cutting forces, in line with the lower roughness shown on the machined surface, when compared to the coated tool with −90 V bias.

Keywords: bias voltage; coated tools; TiAlTaN; tool wear; AISI P20 steel; milling; hard coatings; surface roughness; sustainable manufacturing

1. Introduction

Despite the continuous developments and innovation of new manufacturing processes, the injection mould industry remains a fundamental pillar in today's industry, responsible for more than 30% of plastics produced [1], ensuring a mass-scale production with high-quality standards. Therefore, to endure a competitive manufacturing technology and to stay aligned with the developments of the market, the injection moulding industry needs continuous improvement [2–4], providing solutions that bring sustainability into the process and quality improvement being appreciated, especially by the modern industry [5,6].

Thus, researchers are trying to develop technologies that enhance the mold manufacturing process, causing a positive impact on the life cycle of the plastic injection industry. Therefore, in the last years, thin films have been

studied to be applied by PVD (Physical Vapour Deposition) or CVD (Chemical Vapour Deposition) in end mill tools as a coating [7,8] to enhance their mechanical properties and the moulds surface quality. TiN, TiCN and AlTiN films are usually characterized for their wide application on tools, configuring properties such as high hardness, thermal resistance and wear endurance [9–11], similar to other hard surface coating such as boriding which has recently being studied extensively to improve tribological properties of various additively manufactured alloys [12–16]. Increasing the tool lifespan and the machining performance, better results in terms of surface quality of moulds can be achieved, by a reduction on the vibrations faced by the tool during machining [17–19]. Despite the results achieved by TiN, TiCN and AlTiN, researchers have taken a step forward by adding doping agents such as Si, Cr, Ta, Y to obtain coatings capable of providing even better machining performance [20–24]. This is an aspect of extreme relevance since moulds are manufactured with pre-treated steels, like the AISI P20, which are associated with machining challenges due to their high strength and thermal properties [25].

The bias voltage constitutes a parameter that directly impacts the mechanical properties and morphology of deposited coatings, driving researchers to thoroughly explore the bias influence on the coating properties and consequently on the machining performance [26,27].

Dias et al. [28] applied a direct current that increases from −60 V to −100 V, and with a voltage step to 140 V during the deposition process to ensure the adhesion of the substrate on the tool, demonstrating that bias influence the content of Ta on TiAlTaN coatings and the respective hardness. Pfeiler et al. [29] had researched the influence of bias voltage on the tribological properties of TiAlTaN coatings. Moreover, tribological properties improve due to the phase structure transformation pushed by the bias voltage. On TiAlN based coatings, Cao et al. [30] revealed that with the increment of the bias voltage, the coating atom orientation changes from (200) plane to (111), achieving better results for 75 V, exhibiting 30.3 GPa hardness. For similar hardness levels, Sui et al. [31] in their study, demonstrated that for higher values of Ta, the films possess a columnar structure with superior refinement and higher compactness, influencing the hardness of the coating, achieving values for 31.2 GPa for y = 0.21 Ta content. Sun et al. [32] doped TiAlN substrates with Ta and Si, applying before the deposition process an Argon-ion-etching method using −170 V bias voltage and then depositing the coating at −40 V, resulting in $Ti_{0.42}Al_{0.43}Si_{0.09}Ta_{0.06}N$ better thermal stability and hardness of 37.9 GPa. In other hand, Liu et al. [33] adopted a different strategy by using two different bias cycles to coat the tools, on the first, the values assume 100 V and in the second 150 V and 175 V for a different holding time, concluding that different strategies impact the tribological properties of TiAlN and TiAlSiN coatings. Not adopting distinct cycles, but the same cycle for different bias voltages, Elmkhah et al. [34] reported bias voltage influence in the mechanical properties variation within the TiAlN coating, achieving better results for −100 V. Zhao et al. [35] studied the bias voltage influence on the milling performance of $Ti_{0.33}Al_{0.67}N$ coated tools, concluding that −40 V is the film that presents higher toughness, which makes the film more resilient to crack propagation. In contrast, for higher bias voltages, −120 V, the coating has superior hardness and plasticity. Comparing the two results, the author demonstrated that resistance to crack propagation is more effective in achieving better milling performance. Despite the widespread use of TiAlTaN coatings in machining, few systematic studies have evaluated the influence of bias voltage on the resulting machining performance during PVD deposition, particularly regarding cutting forces and surface roughness. Most existing studies focus on composition or general deposition parameters, leaving the specific role of bias voltage under-explored. As tool lifespan is directly linked to machining quality and sustainability, understanding the effect of bias voltage is scientifically and industrially significant. The objective of this study is to correlate the performance of cutting forces and surface roughness under different levels of bias, using milling tools coated with TiAlTaN.

2. Methodology and Materials

### 2.1. Machining process, Material and Tooling

In the machining process, a 5-axis DMU 60 eVo CNC machining centre, manufactured by Deckel Maho, was employed. For the experimental setup, two sets of five tools were used in conjunction with a lubricating fluid, Alusol SL 51 XBB, comprising 7% oil and 93% water, with the purpose of mitigating adhesive wear phenomena. The use of this lubricant contributed to reduced tool wear and enhanced the surface finish quality of the AISI P20 steel, leading to a decrease in surface roughness and cutting temperature. Regarding the cutting parameters, the following conditions were established: 0 metres to 10 metres cutting length with increments of 2 metres, keeping constant cutting speed (Vc) at 125 m/min, feed rate (Vf) at 716 mm/min, depth of cut (ap) at 0.05 mm, and cutting width (ae) at 3 mm. Figure 1 shows the CNC setup used in the tool tests, setup of the Kistler® (i) dynamometer and (ii) stator and the (iii) workpiece AISI P20 material.
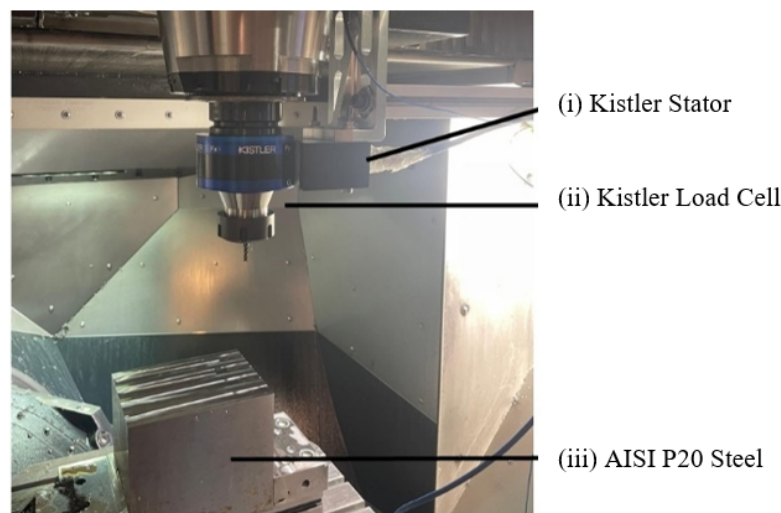
Figure 1. CNC machining set-up during the milling operation in the AISI P20 steel.

During the machining process, the cutting forces were measured using a KISTLER 9171A component dynamometer coupled to a KISTLER 5697A1 data acquisition system. This setup allowed to measure the forces in the X, Y, and Z directions, as well as the torque (Mz), to be recorded using dedicated software. The equipment was mounted on the spindle of the CNC machining center with the appropriate tool clamping system.

This study seeks to help the industry, namely the plastic molding industry. For this reason, AISI P20 steel supplied by Moldit Industries®, Oliveira de Azeméis, Portugal, was used. This material is widely used in the manufacture of molds. Thus, this work aims to contribute to the optimization of machining parameters to improve tool lifespan or improve machining processes, in an industrial context. The AISI P20 Steel, in its chemical composition, contains 0.45% C, 0.40% Si, 1.60 Mn, 0.030 P, 0.035 S, 2.10 Cr, 0.25 Mo and 1.20 Ni. Also, the block of steel used measured 150 mm × 200 mm × 200 mm and mechanical properties of Young's modulus, 205 GPa (T = 20 °C); hardness: 290 HB–330 HB. Capable of performing machining operations in high-strength steels, the WC-Co grade 6110 cemented carbide end mill was used (Figure 2), characterized for possessing four cutting edges with a 35°/38° helix angles, and a corner radius of 0.25 mm. To proceed with the objective of this study, the tools were coated using a CC800®/9 ML CemCon PVD reactor by Durit Coatings®, Coimbra, Portugal, with the application of unbalanced magnetron PVD DC sputtering technology for a bias of −90 V and −135 V, together with targets containing 8% of Ta as dopant, achieving a relation between hardness and Young's modulus of 0.04452 and 0.046135, for −90 V and −135 V, respectively. The average thickness obtained from the coatings on the tools was 3.5 μm.
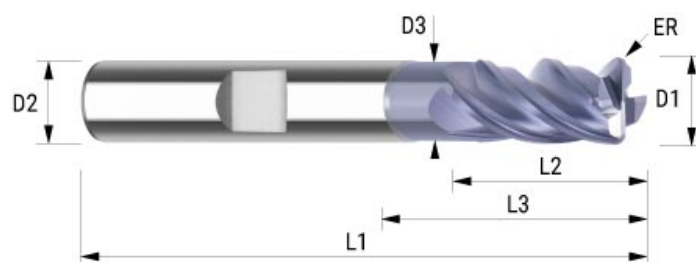
Figure 2. WC-CO grade 6110 carbide milling cutter tool.

Table 1 presents the main dimensions of the tools used during the tests.

Table 1. Main dimensions of the cutting tools [mm].

Diameter	Shaft Diameter	Length of Cut	Total Length	Diameter Release	Releasing Length	Coner Radius	Flutes
D1	D2	L2	L1	D3	L3	ER	Z
4.00	6.00	11	57	3.70	21	0.25	4

2.2. Analysis of Machined Surface Roughness

To identify the cutting parameters that best suit the tools employed in this study, balance process efficiency and reduced wear, such as scratch of tool surface, a cut-off value of 0.8 mm and a measurement length of 5.6 mm were used to record the average surface roughness. Measurements were carried out using a Mahr Perthometer M1 profilometer (Mahr, Göttingen, Germany), under the relevant standard ISO 4288:1996 [36], thereby ensuring the reliability of the results.
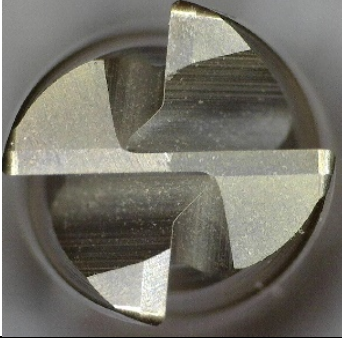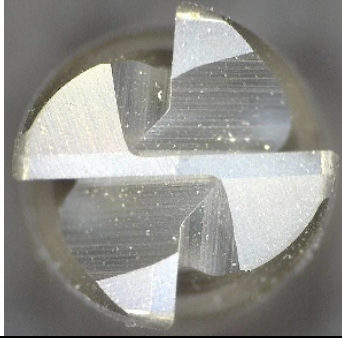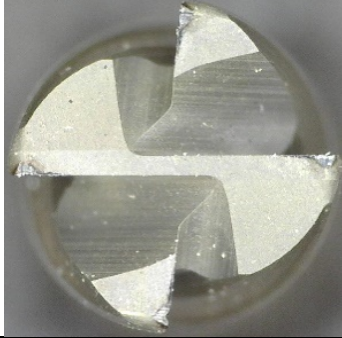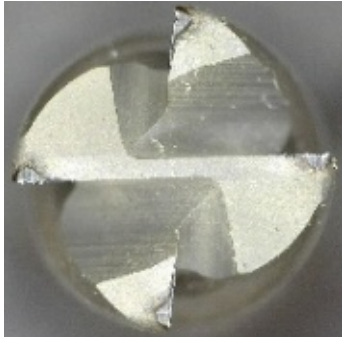
2.3. Tool Wear Analysis Using Optical Microscopy

Tool wear analysis, like Flank wear, chipping, and scratch of tool, was conducted using a Dino-Lite® Edge digital microscope (model WF4915ZT), capable of up to 220× magnification, following the procedures outlined in the ISO 8688-2 standard [37].

3. Results and Discussion

To assess the tools' performance during the milling of AISI P20 steel, their deterioration was carefully examined through the analysis of images obtained via optical microscopy. Table 2 presents top-view images of both coated tools with −90 V and −135 V bias at various cutting length intervals.

Table 2. Optical microscope images of the tools after milling.

TiAlTaN Bias −90 V Tools	TiAlTaN Bias −135 V Tools	Tool Deterioration Phenomena
		Non-machined tools
Cutting length [m] 0	0	
		TiAlTaN Tool, bias −90 V, with 4 m cutting length: Localized chipping. TiAlTaN Tool, bias −135V, with 6 m cutting length: Localized flank wear.
Cutting length [m] 4	6	
		TiAlTaN Tool, bias −90 V: several chipping. TiAlTaN Tool, bias −135V: Localized chipping.
Cutting length [m] 10	10	

Upon analysis of the results obtained, a clear progression of tool wear throughout the machining operation can be observed. However, this wear does not occur at a constant rate. A detailed examination of the tools across different cutting length intervals (0–2 m, 0–4 m, 0–6 m, 0–8 m, and 0–10 m) reveals that, for the tool coated at a −90 V bias, the wear rate is more pronounced within the 0–4 m interval. In contrast, for the tool coated at −135 V, the wear rate is more significant over a longer range, specifically from 0–6 m.

Comparing the two coatings, higher cutting forces were observed for the coating produced with a bias of −90 V. This phenomenon may be attributed, in the author's view, to an initial adaptation period between the AISI P20 steel tool and the characteristics of the tool coating. It may be at this stage, when the edges are broken, that the cutting process becomes more unstable. After this accommodation phase, wear rate becomes more gradual for both tools. In addition to this factor, as noted by other authors, lubricating oxides tend to form on the tool surface only at elevated temperatures [24]. This may further explain the variation in wear rates, as the tool gradually heats up during machining and may eventually reach the temperatures necessary for oxide formation.

Regarding the influence of bias voltage on tool wear, it can be stated that a bias voltage of −135 V results in lower overall wear. This is supported by the comparative images of tool wear at the end of testing, Table 2, which show that the cutting edges of the tool coated at −135 V are better preserved compared to those of the −90 V coated tool. This suggests that higher bias voltages may enhance tool lifespan. The likely reason behind this behaviour lies in the fact that films deposited at higher bias voltages exhibit a higher hardness/Young's modulus ratio (as described in the methodology section), which directly influences wear mechanisms.

When comparing the two tools, abrasive wear of the coating was observed in both cases; however, chipping was more frequently encountered during the operation of the −90 V coated tool. This aligns with the lower hardness to Young's modulus ratio associated with the −90 V coating in comparison to the −135 V. The values related to cutting forces resulting from the tests are presented in Figure 3. In Figure 3a the cutting forces can be seen with a coated tool with a bias of −90 V and Figure 3b with a coated tool with a bias of −135 V.

Following the previously outlined methodology, the cutting force values were computed and graphically represented following the acquisition of cutting forces data from the cutting tool. Preliminary analysis of the resulting plots suggests that cutting forces are influenced by the extent of tool wear and the type of coating applied.

Figure 3a shows that for the TiAlTaN-coated tool at a bias voltage of −90 V, the evolution of cutting forces is nonlinear, mirroring the tool's wear progression. Initially, a cutting force of 16.8 N is recorded, gradually increasing to around 18 N before reaching a peak value of 21.49 N. A slight decline is then observed, stabilising at approximately 20.99 N over the subsequent 250 s. This trend can be explained by examining the observed wear mechanisms. The initial increase in force up to 18 N corresponds to an adaptation phase between the tool coating and the AISI P20 workpiece material, during which abrasive wear predominates.

After analysing Figure 3a, it can be seen that a more accelerated wear process is initiated, most notably between 200 and 400 s. However, the mechanical consequences only become apparent after this time. The cumulative effects of abrasion and coating chipping contribute to the abrupt increase in cutting force as the cutting edges of the tool become dull and material begins to detach. Following this degradation phase, the cutting force profile stabilises between 400 and 600 s, which is consistent with a post-critical wear regime in which the tool has experienced significant degradation.

Regarding the tool coated with TiAlTaN at a bias voltage of −135 V, Figure 3b, the cutting force behaviour exhibits a broadly similar trend to that of the −90 V tool, albeit with notable differences. Initially, a cutting force of 14.3 N is recorded, followed by a gradual increase to 14.68 N after 60 s. Over the subsequent 300 s, the cutting force continues to rise progressively, reaching approximately 15 N. This is followed by a more pronounced increase, peaking at 16.5 N, preceded by a slight drop of 0.5 N. After this point, the cutting force stabilises.

A direct comparison of the two tools shows clear differences in both the magnitude of the cutting forces and their rate of evolution over time. Regarding wear progression, the tool coated at −135 V showed a more gradual increase in cutting forces throughout the test. Furthermore, during the time interval in which both tools experienced the most significant wear, the −135 V coated tool did not display as sharp a rise in cutting force. This behaviour is primarily attributed to the dominant wear mechanisms at the tool edges. In the case of the −135 V tool, chipping was less frequent, and abrasive wear was the predominant mode. Additionally, when comparing the initial and final cutting force values, the increase observed for the −135 V tool was only 1.7 N. In contrast, the −90 V tool exhibited a rise of 4.17 N, three times more than the −135 V tool. This finding is consistent with the conclusions previously outlined in this study, which indicated a higher degree of final tool wear for the −90 V, attributed to the differences in mechanical strength and hardness of the respective coatings.

The surface roughness of the AISI P20 steel was measured at the end of each 2-metre cutting length interval to assess the impact of the performance of each end mill on the surface quality of the machined component.

Pinto et al.

J. Mech. Eng. Manuf. **2025**, *1*(1), 7

As can be seen in Figure 4, the surface roughness values were consistently lower for the tool coated at a bias voltage of −135 V. Examining the roughness evolution throughout the test revealed a similar trend for both tools. Initially, a roughness value was recorded for the first interval, followed by a decrease in roughness in the second (2–4 m) interval. In subsequent intervals, roughness values increased progressively, ultimately reaching higher final values.


(a)

(b)
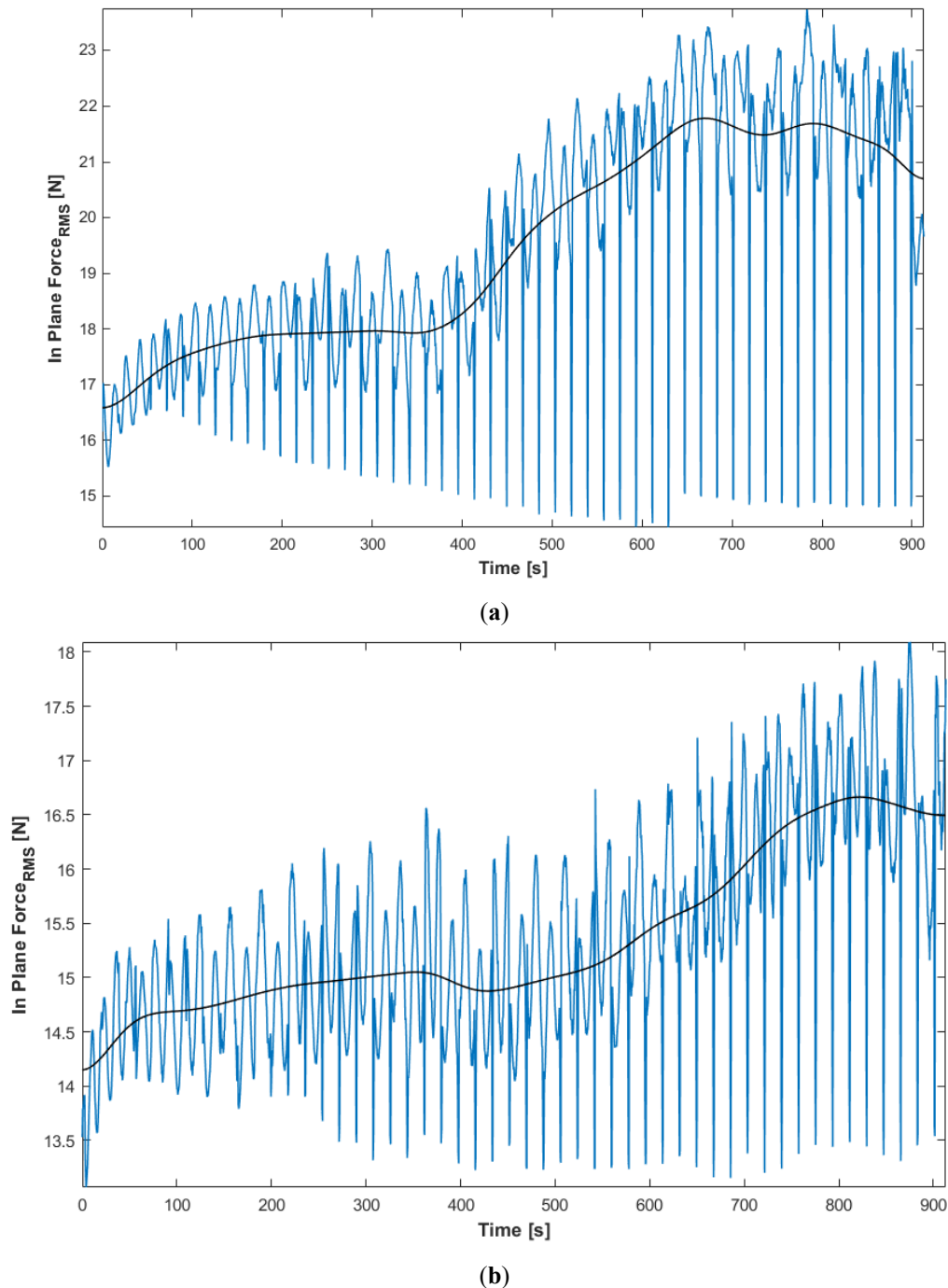
Figure 3. **(a)** Tool with TiAlTaN coating −90 V bias, 0–10 Cutting lengths [m]; **(b)** Tool with TiAlTaN coating −135 V bias, 0–10 Cutting lengths [m].

From a correlation standpoint, a direct relationship between the evolution of surface roughness and cutting forces is evident. As shown in Table 3, the total increase in roughness occurred predominantly between 0–4 m for the −90 V tool, and between 0–6 m for the −135 V tool. Furthermore, consistent with the cutting force trends, the most significant increase in roughness for the −90 V tool was observed between 2–4 m. In contrast, the tool coated

at −135 V demonstrated a more gradual increase in surface roughness across the 2–6 m interval, which is consistent with a more progressive wear mechanism.
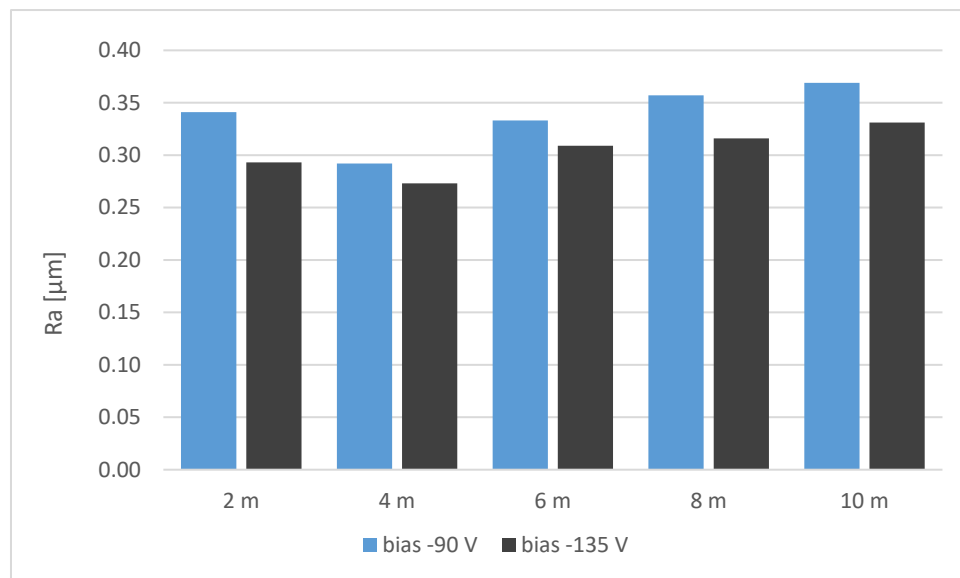
Figure 4. Roughness values during test for TiAlTaN −90 V and TiAlTaN −135 V coatings.

Table 3. Average values of Ra and maximum cutting force regarding the three tools tested for TiAlTaN −90 V and TiAlTaN −135 V coatings.

Cutting Length Interval [m]	TiAlTaN −90 V		TiAlTaN −135 V	
	Ra [µm]	Maximum Cutting Force [N]	Ra [µm]	Maximum Cutting Force [N]
0–2	0.341	16.82	0.293	14.68
0–4	0.292	17.98	0.273	14.93
0–6	0.333	20.48	0.309	15.03
0–8	0.357	21.42	0.316	16.07
0–10	0.369	20.99	0.331	16.38

Based on this roughness evaluation, it can be concluded that films deposited at −135 V bias exhibit superior performance compared to those coated at −90 V. This improves the surface finish of the machined material AISI P20 and contributes to longer tool lifespan. The results obtained in this study are consistent with previous findings, particularly those reported by Pinto G. [27] and Baptista [26]. Both studies investigated the influence of bias voltage on TiAlYN and TiAlTaN coatings: Pinto G. used DC sputtering while Baptista used the HiPIMS technique. In both cases, a bias voltage of −135 V was identified as the optimal parameter, resulting in denser and harder coatings, improved adhesion, and lower surface roughness. These coatings also exhibited better resistance to friction and reduced wear, while maintaining the crystalline structure of the thin film. Additionally, Pinto G. also tested different cutting speeds and found that the highest speed (125 m/min) resulted in improved tool performance. Andresa Baptista evaluated the influence of feed rate during machining and observed similar trends in tool performance. These consistent results reinforce the critical role of bias voltage in enhancing coating properties and machining performance, regardless of the deposition technique employed. Also, the results presented in this study demonstrate that adding the Ta dopant to the TiAlN base coating improves cutting forces and increases tool lifespan, according to Tillmann et al. [38].

4. Conclusions

This study allowed the correlation between cutting performance and surface roughness to be investigated under different preloads using TiAlTaN coated end mills. By acquiring the cutting forces, it was confirmed as expected, these increases occur throughout the machining cycle. However, it became evident that the tool coated at −135 V consistently exhibited lower cutting force values compared to the −90 V variant. This finding aligns with observations made via optical microscopy of the tool cutting edges, which revealed more severe wear and a greater occurrence of chipping in the −90 V tool. This degradation leads to a reduction in cutting efficiency, as the worn edges become less sharp and less effective in removing material, particularly critical when machining

challenging materials such as AISI P20 steel. By correlating the wear rate with cutting force evolution, it can be concluded that the −135 V coated tool offers a longer lifespan and superior cutting performance.

These mechanical advantages translated directly into surface quality improvements, as shown by the surface roughness analysis. Specifically, the −135 V coated tool produced a lower final surface roughness of 0.331 μm Ra, compared to 0.369 μm Ra for the −90 V tool. Therefore, in machining operations where surface finish is a critical performance parameter, the use of TiAlTaN coated tools deposited at a −135 V bias voltage is strongly recommended.

For future work, it would be interesting to evaluate a wider range of polarisation voltages. When working with higher voltages in a module, attention must be paid to the crystalline structure. Amorphous structures should be avoided because they lose their mechanical properties, which weakens the thin film.

Author Contributions

A.B., G.F.P.: conceptualization; A.B., G.F.P.: methodology; D.A.: writing-original draft preparation; A.B., G.F.P., F.F.: investigation; F.J.G.S.: supervision; E.S., R.A. validation; F.J.G.S., A.B., G.F.P.: writing-reviewing and editing. All authors have read and agreed to the published version of the manuscript.

Funding

Institutional Review Board Statement

Not applicable.

Informed Consent Statement

Not applicable.

Data Availability Statement

Not applicable.

Conflicts of Interest

The authors declare no conflict of interest.

References

1. Schubert, M.; Perfetto, S.; Dafnis, A.; et al. *Multifunctional Load Carrying Lightweight Structures for Space Design*; Deutsche Gesellschaft für Luft-und Raumfahrt: Bonn, Germany, 2017.
2. Stampone, B.; Pulcini, V.; Vitale, G.; et al. *Towards Industry 5.0 within Micro-Injection moulding Production and Industrialisation: A proof of concept. Procedia Comput. Sci.* **2025**, *253*, 3007–3014.
3. Farooque, R.; Asjad, M.; Rizvi, S.J.A. A current state of art applied to injection moulding manufacturing process—A review. *Mater. Today Proc.* **2021**, *43*, 441–446.
4. Párizs, R.D.; Török, D.; Ageyeva, T.; et al. Machine Learning in Injection Molding: An Industry 4.0 Method of Quality Prediction. *Sensors* **2022**, *22*, 2704.
5. Silva, B.; Marques, R.; Faustino, D.; et al. Enhance the Injection Molding Quality Prediction with Artificial Intelligence to Reach Zero-Defect Manufacturing. *Processes* **2023**, *11*, 62.
6. Pozzi, R.; Rossi, T.; Secchi, R. Industry 4.0 technologies: critical success factors for implementation and improvements in manufacturing companies. *Prod. Plan. Control.* **2023**, *34*, 139–158.
7. Baptista, A.; Silva, F.; Porteiro, J.; et al. Sputtering Physical Vapour Deposition (PVD) Coatings: A Critical Review on Process Improvement and Market Trend Demands. *Coatings* **2018**, *8*, 402.
8. Baptista, A.; Porteiro, J.; Míguez, J.L.; et al. On the Physical Vapour Deposition (PVD): Evolution of Magnetron Sputtering Processes for Industrial Applications. *Procedia Manuf.* **2018**, *17*, 746–757.
9. Çalışkan, H.; Küçükköse, M. The effect of aCN/TiAlN coating on tool wear, cutting force, surface finish and chip morphology in face milling of Ti6Al4V superalloy. *Int. J. Refract. Met. Hard Mater.* **2015**, *50*, 304–312.
10. Bouzakis, A.; Skordaris, G.; Bouzakis, E.; et al. Wear Evolution on PVD Coated Cutting Tool Flank and Rake Explained Considering Stress, Strain and Strain-Rate Dependent Material Properties. *Coatings* **2023**, *1982*, 13.

11. Sousa, V.F.C.; Da Silva, F.J.G.; Pinto, G.F.; et al. Characteristics and Wear Mechanisms of TiAlN-Based Coatings for Machining Applications: A Comprehensive Review. *Metals* **2021**, *11*, 260.

12. Girisken, I.; Cam, G. Characterization of microstructure and high-temperature wear behavior of pack-borided Co-based Haynes 25 superalloy. *CIRP J. Manuf. Sci. Technol.* **2023**, 45, 82–98. https://doi.org/10.1016/j.cirpj.2023.06.012.

13. Gunen, A.; Gurol, U.; Kocak, M.; et al. Investigation into the influence of boronizing on the wear behavior of additively manufactured Inconel 625 alloy at elevated temperature. *Prog. Addit. Manuf.* **2023**, 8, 1281–1301. https://doi.org/10.1007/s40964-023-00398-8.

14. Gunen, A.; Gurol, U.; Kocak, M.; et al. A new approach to improve some properties of wire arc additively manufactured stainless steel components: Simultaneous homogenization and boriding. *Surf. Coat. Technol.* **2023**, 460, 129395. https://doi.org/10.1016/j.surfcoat.2023.129395.

15. Kocaman, E.; Gurol, U.; Gunen, A.; et al. Effect of post-deposition heat treatments on high-temperature wear and corrosion behavior of Inconel 625. *Mater. Today Commun.* **2025**, *42*, 111101. https://doi.org/10.1016/j.mtcomm.2024.111101.

16. Cam, G.; Gunen, A. Challenges and opportunities in the production of magnesium parts by directed energy deposition processes. *J. Magnes. Alloys* **2024**, *12*, 1663–1686. https://doi.org/10.1016/j.jma.2024.05.004.

17. Bejaxhin, A.B.H.; Paulraj, G. A Review on Effect of Coatings on Tools and Surface Roughness as Vibration Resistance. *Int. J. Emerg. Technol. Eng. Res.* **2017**, *5*, 50–57.

18. Saruhan, H.; Yıldız, M. Experimental Vibration Analysis of Titanium Aluminum Nitride (TiAlN) Coated Milling Cutting Tool Effects on Surface Roughness of AISI 4140 Steel Products. *Duzce Univ. J. Sci. Technol.* **2018**, *6*, 745–753.

19. Sousa, V.F.C.; Silva, F.J.G.; Alexandre, R.; et al. Study of the wear behaviour of TiAlSiN and TiAlN PVD coated tools on milling operations of pre-hardened tool steel. *Wear* **2021**, *476*, 203695.

20. Alhafian, M.R.; Valle, N.; Chemin, J.B.; et al. Influence of Si addition on the phase structure and oxidation behavior of PVD AlTiN and AlTiCrN coatings using high-resolution characterization techniques. *J. Alloys Compd.* **2023**, *968*, 171800.

21. Fang, C.; Zhang, C.; Zhu, S.; et al. The influence of Y additions on the microstructure and mechanical properties of MoTaWNb refractory high entropy alloy films by magnetron sputtering. *Surf. Coat. Technol.* **2024**, *484*, 130792.

22. Gordon, S.; Rodriguez-Suarez, T.; Roa, J.J.; et al. Mechanical integrity of PVD TiAlN-coated PcBN: Influence of substrate bias voltage and microstructural assemblage. *Ceram. Int.* **2024**, *50*, 6299–6308.

23. Yang, W.; Xiong, J.; Guo, Z.; et al. Structure and properties of PVD TiAlN and TiAlN/CrAlN coated Ti(C, N)-based cermets. *Ceram. Int.* **2017**, *43*, 1911–1915.

24. Aninat, R.; Valle, N.; Chemin, J.B.; et al. Addition of Ta and Y in a hard Ti-Al-N PVD coating: Individual and conjugated effect on the oxidation and wear properties. *Corros. Sci.* **2019**, 156, 171–180.

25. Abbas, A.T.; Sharma, N.; Alsuhaibani, Z.A.; et al. Multi-Objective Optimization of AISI P20 Mold Steel Machining in Dry Conditions Using Machine Learning. *Machines* **2023**, *11*, 748.

26. Baptista, A. Efficiency, Coating Properties, and Machining Performance of Thin Films Deposited Using HiPIMS: An Experimental Analysis. Ph.D. Thesis, University of Vigo, Vigo, Spain, 2024, https://doi.org/10.35869/11093/8887.

27. Pinto, G.F. Experimental Study on PVD DC Sputtering Thin Films: Efficiency, Coating Properties, and Wear Tools Performance on Milling Pre-Hardness Tools Steels. Ph.D. Thesis, University of Vigo, Vigo, Spain, 2024, https://doi.org/10.35869/11093/8885.

28. Dias, N.F.L.; Meijer, A.L.; Biermann, D.; et al. Structure and mechanical properties of TiAlTaN thin films deposited by dcMS, HiPIMS, and hybrid dcMS/HiPIMS. *Surf. Coat. Technol.* **2024**, *487*, 130987.

29. Pfeiler, M.; Fontalvo, G.A.; Wagner, J.; et al. Arc Evaporation of Ti–Al–Ta–N Coatings: The Effect of Bias Voltage and Ta on High-temperature Tribological Properties. *Tribol. Lett.* **2008**, *30*, 91–97.

30. Cao, H.-S.; Liu, F.-J.; Li, H.; et al. Effect of bias voltage on microstructure, mechanical and tribological properties of TiAlN coatings. *Trans. Nonferrous Met. Soc. China* **2022**, *32*, 3596–3609.

31. Sui, X.; Li, G.; Jiang, C.; et al. Effect of Ta content on microstructure, hardness and oxidation resistance of TiAlTaN coatings. *Int. J. Refract. Met. Hard Mater.* **2016**, *58*, 152–156.

32. Sun, X.; Liu, Z.R.; Chen, L. Influence of Si and Ta mixed doping on the structure, mechanical and thermal properties of TiAlN coatings. *Surf. Coat. Technol.* **2023**, *461*, 129428.

33. Liu, X.; Zhang, H.; Liu, C.; et al. Influence of bias patterns on the tribological properties of highly hydrogenated PVD a-C:H films. *Surf. Coat. Technol.* **2022**, *442*, 128234.

34. Elmkhah, H.; Zhang, T.F.; Abdollah-zadeh, A.; et al. Surface characteristics for the TiAlN coatings deposited by high power impulse magnetron sputtering technique at the different bias voltages. *J. Alloys Compd.* **2016**, *688*, 820–827.

35. Zhao, B.; Zhao, X.; Lin, L.; et al. Effect of bias voltage on mechanical properties, milling performance and thermal crack propagation of cathodic arc ion-plated TiAlN coatings. *Thin Solid Film.* **2020**, 708, 138116.

36. *ISO 4288:1996*; Geometrical Product Specifications (GPS)—Surface Texture: Profile Method—Rules and Procedures

for the Assessment of Surface Texture. International Organization for Standardization: Geneva, Switzerland, 1996.

37. *ISO 8688-2:1989*; Tool Life Testing in Milling—Part 2: End Milling. International Organization for Standardization: Geneva, Switzerland, 1989.

38. Tillmann, W.; Meijer, A.L.; Platt, T.; et al. Cutting performance of TiAlN-based thin films in micromilling high-speed steel AISI M3:2. *Manuf. Lett.* **2024**, *40*, 6–10. https://doi.org/10.1016/j.mfglet.2024.01.005.